APPLICATION OF THE SCHWARZ-CHRISTOFFEL TRANSFORMATION IN SOLVING TWO-DIMENSIONAL TURBULENT FLOWS IN COMPLEX GEOMETRIES

R. Moosavi

Department of Mechanical Engineering, Yasouj University
P.O. Box 75914, Yasouj, Iran
rmoosavi81@gmail.com

S.A. Gandjalikhan Nassab*

Department of Mechanical Engineering, Shahid Bahonar University
P.O. Box 76169-133, Kerman, Iran
ganjali2000@yahoo.com

*Corresponding Author

(Received: March 12, 2008 – Accepted in Revised Form: September 25, 2008)

Abstract In this paper, two-dimensional turbulent flows in different and complex geometries are simulated by using an accurate grid generation method. In order to analyze the fluid flow, numerical solution of the continuity and Navier-Stokes equations are solved using CFD techniques. Considering the complexity of the physical geometry, conformal mapping is used to generate an orthogonal grid by means of the Schwarz-Christoffel transformation. The standard k-ε turbulence model is employed to simulate the mean turbulent flow field, using a linear low-Re k-ε model for near wall region. The governing equations are transformed in the computational domain and the discretized forms of these equations are obtained by the control volume method. Finite difference forms of the governing equations are solved in the computational plane and the SIMPLE algorithm is used for the pressure-velocity coupling. The important part of the present work is based on the numerical integration of Schwraz-Christoffel transformation in grid generation for simulating fluid flow in different complex geometries. To validate the computational results, the theoareticil data is compared with that of theoretical results achieved by other investigators, which are in reasonable agreement.

Keywords Schwarz-Christoffel Transformation, Grid Generation, Turbulent Flow

چکیده در این مقاله نمونه هایی از جریان های دو بعدی آشفته و غیر قابل تراکم با هندسه های پیچیده و متفاوت با بکارگیری تکنیک دینامیک سیالات محاسباتی (CFD) حل شده اند. یکی از مهمترین قسمت ها در روش حل عددی جریان سیال، تولید شبکه محاسباتی است که در کار حاضر از طریق نگاشت همدیس و استفاده از تابع تبدیل شوارتز-کریستوفل به انجام رسیده است. روش نگاشت همدیس استفاده شده مبتنی بر انتگرال گیری عددی از تبدیل شوارتز-کریستوفل می‌باشد. از مزایای این روش می‌توان به سادگی و دقت زیاد آن در عین توانایی قابل ملاحظه در تولید شبکه با هندسه پیچیده اشاره کرد. در این مطالعه به منظور شبیه سازی جریان سیال ،حل عددی معادلات پیوستگی و ناویر-استوکس بصورت هم زمان انجام شده و از مدل توربولانس k-ε استاندارد برای محاسبه تنش های ناشی از نوسانات سرعت به همراه یک مدل خطی برای نواحی نزدیک دیواره استفاده شده است. به این ترتیب که معادلات حاکم به صفحه محاسباتی منتقل گردیده و با روش حجم محدود مجزا سازی شده اند و نهایتا فرم اختلاف محدود این معادلات توسط آلگوریتم شناخته شده سیمپل بصورت عددی حل شده است. مطابقت نزدیک بین پیش بینی های روش حاضر و نتایج تئوریک و تجربی دیگران مویدصحت روش بکار گرفته شده در تولید شبکه و حل عددی معادلات حاکم می‌باشد.

1. INTRODUCTION

The numerical solution of many problems such as fluid flow consists in discretizing the domain upon which the governing equations must be solved. These equations are linearized inside small control volumes where the conservation equations are applied. The fast increase in computer technology and data storage have led to the application of Computational Fluid Dynamic (CFD) in simulation of laminar and turbulent flows with different geometries. The application of CFD methods need to have a discretized region and it is of great importance to be able to generate grid. The methods of generating mesh in the domains with arbitrary boundaries are divided to, algebraic and differential methods and both orthogonal and non-orthogonal grids can be generated. Normally, for all numerical methods, it is better that the generated grid is structured and orthogonal. In orthogonal grid, the coordinate lines are mutually perpendicular to each other. In this type of grid, it is an easier application of boundary conditions involving the normal derivatives to the boundaries. Besides, the transformed forms of governing equations in the computational domain with orthogonal grid have less number of terms in comparison to the non-orthogonal case.

One of the accurate method in orthogonal grid generation without any restriction on the type of flow, is the conformal mapping technique [1-3]. In practice, the generated grid lines which are perpendicular to each other may be chosen to coincide with the streamlines and equipotential lines of an equivalent potential flow problem.

Several efficient methods have been developed using the conformal mapping technique to obtain two-dimensional meshes. Traditionally many times, this technique has been used to carry out the solution of potential flow about complicated geometrical shapes [4]. Mansouri, et al [5] used simple mapping in orthogonal grid generation for external flows over bodies with a variety of shapes. In another work by the same investigators, some potential flows over bodies with different geometries were simulated in which the mesh generation was done using the Schwarz-Christoffel transformation [6].

In the present work, two-dimensional turbulent flows over some bodies with different and complex geometries are simulated using orthogonal grid generated by conformal mapping technique. The mapping of physical plane into computational one takes place by the Schwarz-Christoffel transformation. The governing equations consisting of the continuity and Navier-Stokes equations with the equations governing the kinetic energy of turbulence and the dissipation rate are transformed in the computational plane and solved by CFD techniques. To calculate the values of Reynolds stresses, combination of the standard k-ε turbulence model and a linear low-Re k-ε one for near wall region is employed.

2. THEORY

2.1. Mean Flow Equations The conservations of mass and momentum for a steady incompressible two-dimensional turbulent flow may be written as:

Continuity

$$\frac{\partial U_j}{\partial x_j} = 0 \tag{1}$$

Momentum

$$\frac{\partial (U_j U_i)}{\partial x_j} = -\frac{1}{\rho}\frac{\partial P}{\partial x_i} + \frac{\partial}{\partial x_j}\left(\nu \frac{\partial U_i}{\partial x_j} - \overline{u_i u_j}\right) \tag{2}$$

in which U_j are the mean velocity components and $\overline{u_i u_j}$ are the Reynolds stresses.

2.2. Turbulence Model Equations The turbulence model employed in the simulation of turbulent flow is the standard k-ε model [7]. In this turbulence model, the Reynolds stresses are calculated via the eddy-viscosity approximations as follows:

$$\overline{u_i u_j} = -\nu_t\left(\frac{\partial U_i}{\partial x_j} + \frac{\partial U_j}{\partial x_i}\right) + \frac{2}{3}\delta_{ij} k \tag{3}$$

and the turbulent viscosity, ν_t, is given by

$$\nu_t = c_\mu \frac{k^2}{\varepsilon} \tag{4}$$

In which the turbulent kinetic energy k and turbulent dissipation rate ε are obtained based on the standard k-ε model from the following transport equations:

$$\frac{\partial}{\partial x_j}(U_j k) = \frac{\partial}{\partial x_j}[(\frac{\nu_t}{\sigma_k})\frac{\partial k}{\partial x_j}] + P_k - \varepsilon \qquad (5)$$

$$\frac{\partial}{\partial x_j}(U_j \varepsilon) = \frac{\partial}{\partial x_j}[(\frac{\nu_t}{\sigma_\varepsilon})\frac{\partial \varepsilon}{\partial x_j}] + c_{\varepsilon 1}\frac{\varepsilon}{k}P_k - c_{\varepsilon 2}\frac{\varepsilon^2}{k} \qquad (6)$$

Where P_k which is the generation rate of turbulent kinetic energy that can be computed from Equation 7

$$P_k = -\overline{u_i u_j}\frac{\partial U_i}{\partial x_j} \qquad (7)$$

The coefficients in Equations 4 to 6 are given in Table 1.

2.3. Near Wall Region In the present work, for modeling the near-wall region, a linear low-Re k-ε model is employed. In this turbulence model, the turbulent viscosity, ν_t, is obtained from

$$\nu_t = c_\mu f_\mu \frac{k^2}{\tilde{\varepsilon}} \qquad (8)$$

and the transport equations for the turbulence kinetic energy, k, and homogenous dissipation rate, $\tilde{\varepsilon}$ are as follows:

$$\frac{\partial}{\partial x_j}(U_j k) = \frac{\partial}{\partial x_j}[(\nu + \frac{\nu_t}{\sigma_k})\frac{\partial k}{\partial x_j}] + P_k - \tilde{\varepsilon} - 2\nu(\frac{\partial \sqrt{k}}{\partial x_j})^2 \qquad (9)$$

TABLE 1. Empirical Constants for the k-ε Model.

c_μ	$c_{\varepsilon 1}$	$c_{\varepsilon 2}$	σ_k	σ_ε	σ_θ
0.09	1.44	1.92	1	1.3	0.9

$$\frac{\partial}{\partial x_j}(U_j \tilde{\varepsilon}) = \frac{\partial}{\partial x_j}[(\nu + \frac{\nu_t}{\sigma_\varepsilon})\frac{\partial \tilde{\varepsilon}}{\partial x_j}] + c_{\varepsilon 1}\frac{\tilde{\varepsilon}}{k}P_k - \tilde{\varepsilon} - c_{\varepsilon 2} f_2 \frac{\tilde{\varepsilon}^2}{k} + E + S_\varepsilon \qquad (10)$$

The homogeneous dissipation rate and damping factors are calculated from

$$\tilde{\varepsilon} = \varepsilon - 2\nu(\frac{\partial \sqrt{k}}{\partial x_j})^2 \qquad (11)$$

$$f_\mu = 1 - \exp[-(\tilde{R}_t/90)^{0.5} - (\tilde{R}_t/400)^2] \qquad (12)$$

$$f_2 = 1 - 0.3\exp(-\tilde{R}_t^{\,2}) \qquad (13)$$

Where $\tilde{R}_t = k^2/\nu\tilde{\varepsilon}$ is the local turbulent Reynolds number, $P_k = -\overline{u_i u_j}(\partial U_i/\partial x_j)$ the generation rate of turbulent kinetic energy and the term E is defined as

$$E = 2\nu\nu_t(\frac{\partial U_i}{\partial x_j \partial x_k})^2 \qquad (14)$$

and the extra source term S_ε in Equation 10 stands for the standard "Yap" correction term which was introduced first time by Yap, et al [8]. The details of this model with the model coefficients are given by Raisee, et al [9].

2.4. Boundary Conditions In the numerical solution of governing equations, the following boundary conditions in the physical plane are considered:

- At the inlet section or in the upstream region far from body, it is assumed that the fluid flow has a uniform velocity distribution equal to U with turbulent kinetic energy of $k = 0.001U^2$ and dissipation rate of $\varepsilon = \rho C_\mu k^2/\nu_t$ such that $\nu_t/\nu = 10$.

- At the outlet section or in the downstream region far from body, a zero gradient in stream-wise direction is considered for all dependent variables.
- On the solid walls, no slip condition is employed, the turbulent kinetic energy is equated to zero and dissipation rate is computed by [9]:

$$\varepsilon = 2\nu(\partial\sqrt{k}/\partial n)^2 \tag{15}$$

in which n stands for normal direction to the solid surface.

3. GRID GENERATION

As noted before, the grid generation in the present work is based on the numerical integration of the Schwarz-Christoffel transformation. By this transformation, a polygon in the z(x,y)-plane, is mapped onto the upper half of $\gamma(\xi,\eta)$-plane as shown in Figure 1.

The relation between the z-plane as physical domain to the γ-plane as computational one is as follows:

$$\frac{dz}{d\gamma} = A \prod_{n=1}^{N} (\gamma - \xi_n)^{-\alpha_n/\pi} \tag{16}$$

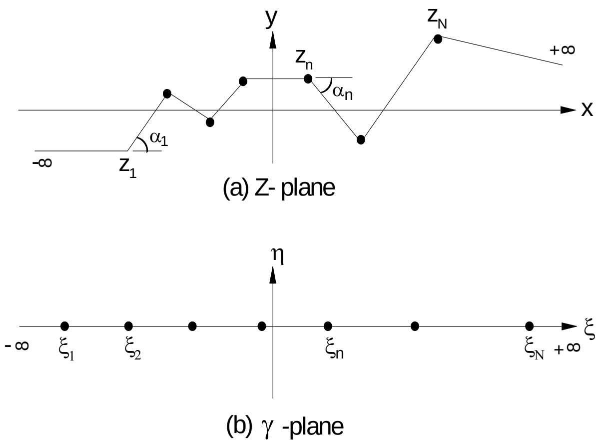

Figure 1. Mapping of a polygon in z(x,y)-plane onto the upper half of $\gamma(\xi,\eta)$-plane.

In the above equation, α_n is the angle of counterclockwise rotation at each apex and N is the number of polygon apices. The points ξ_n are positions on the real axis in γ-plane, where each of them corresponds to an apex of the polygon in z-plane. The values of parameters ξ_n are unknown which will be determined iteraively during the numerical procedure. Also, in Equation 16, A is a complex constant which depends on the geometry of physical domain. According to Riemann theorem, et al [4], the positions of three points of ξ_n at the real axis of computational plane are arbitrary. The transformation function $z(\gamma)$ denoting the relation between physical and computational axes can be obtained by integration of Equation 16 as follows:

$$z(\gamma) = A \int_{\gamma_0}^{\gamma} \prod_{n=1}^{N} (\gamma - \xi_n)^{-\alpha_n/\pi} d\gamma + B \tag{17}$$

In Equation 17, B is a complex constant and γ_0 is a point on the upper half of computational plane. As noted before, the correct selection of points ξ_n involves an iterative procedure. The details of this transformation and the related numerical procedure are given completely in Reference [6]. It must be mentioned in that reference, the Schwarz-Christoffel transformation was used to generate orthogonal grids which also solves some internal and external potential flows in different geometries. But, in the present work, this grid generation technique is employed to simulate viscous turbulent flows in a wide variety of complex geometries. By this technique, the relation between physical and computational planes is determined, from which the values of metric coefficients, which are needed to transform the governing equations into computational domain can be obtained. The transformed form of the governing equations in the computational plane for any dependent variable Ψ, can be written in the following common form:

$$\frac{\partial}{\partial\xi}[JA\Psi - \Gamma_\Psi \frac{\partial\Psi}{\partial\xi}] + \frac{\partial}{\partial\eta}[JB\Psi - \Gamma_\Psi \frac{\partial\Psi}{\partial\eta}] = S_\Psi \tag{18}$$

In which, J is the Jacobian of transformation and the values of A, B, Ψ, Γ_{Ψ} and S_{Ψ} are different for each governing equation.

4. OUTLINE OF SOLUTION STRATEGY

The governing equations which were transformed in the computational plane have a common form as was presented in Equation 18. These partial differential equations were made discrete by integrating over an elemental cell volume using the finite volume methodology. Such that, the staggered type of control volumes for the ξ-and η-velocity components were used when other variables of interest were computed at the grid nodes. The discretized forms of all transport equations were obtained by employing hybrid differencing scheme for approximation of the convective terms in these equations and were solved by the SIMPLE pressure correction algorithm of Patankar, et al [10]. Numerical solutions were obtained iteratively through line-by-line method until the convergence condition was achieved. Iterations were terminated when sum of the absolute residuals was less than 10^{-4} for each equation.

Numerical calculations were coded into a computer program in FORTRAN. Based on the grid-independent study, the optimum grids with 350 to 450 intervals in the ζ-direction and 120 to 180 intervals in the η-direction dependent on the flow geometry were employed for the numerical analysis along with clustering near the solid boundaries and in the regions with sharp gradients. Calculations were run with a Pentium 5 personal computer and the simulation times ranged from 3000 to 4000 secs depending on the test case conditions.

5. RESULTS

To verify the performance and accuracy of the present method and to simulate two-dimensional turbulent flows in different geometries, many test cases of fluid flows over different bodies including forward/backward steps, one and two cylinders, two cubes, two triangular sharp bumps and car profile were analyzed here.

An interesting type of fluid flow is the flow over forward or backward steps. The existence of flow separation and reattachment due to sudden expansion and contraction in these types of geometries, plays an important role in the design of many engineering applications. As the first test case, the fluid flow over double forward facing step (DFFS) was simulated. The basic flow configuration is shown in Figure 2. The channel has two forward facing steps with heights of h_1 and h_2, respectively. H and L are the height and length of the channel, where b, c and a are the length of two steps and the length of bottom wall, respectively.

The stream lines along with the values of stream function for fluid flow over DFFS are shown in Figure 3a. In this figure, the values of geometrical parameters h_1/H, h_2/H, a/L, b/L, and c/L are 0.2, 0.4, 0.625, 0.125 and 0.25, respectively. These data are the same as used in Reference [11] to make a comparison between results. As it is seen, several circulation zones are generated on the facing steps. The variation of pressure coefficient is shown in Figure 3b. In the vicinity of inlet section, the pressure contours are vertical to the bottom and top walls until the first step, which indicates that the fluid flow becomes hydrodynamically developed in that region. The value of pressure coefficient decreases in the flow direction, such that the pressure coefficient at the second step is less than that of the first one. Besides, due to the complexity of flow geometry near the steps, the pressure coefficient has a very complex variation in that region. The contours of turbulent kinetic energy (TKE) are plotted in Figure 3c. TKE has small values near the solid

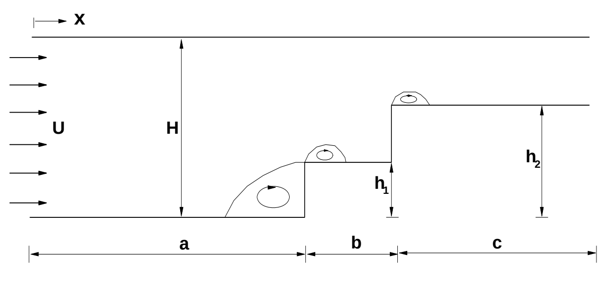

Figure 2. Sketch of the problem geometry.

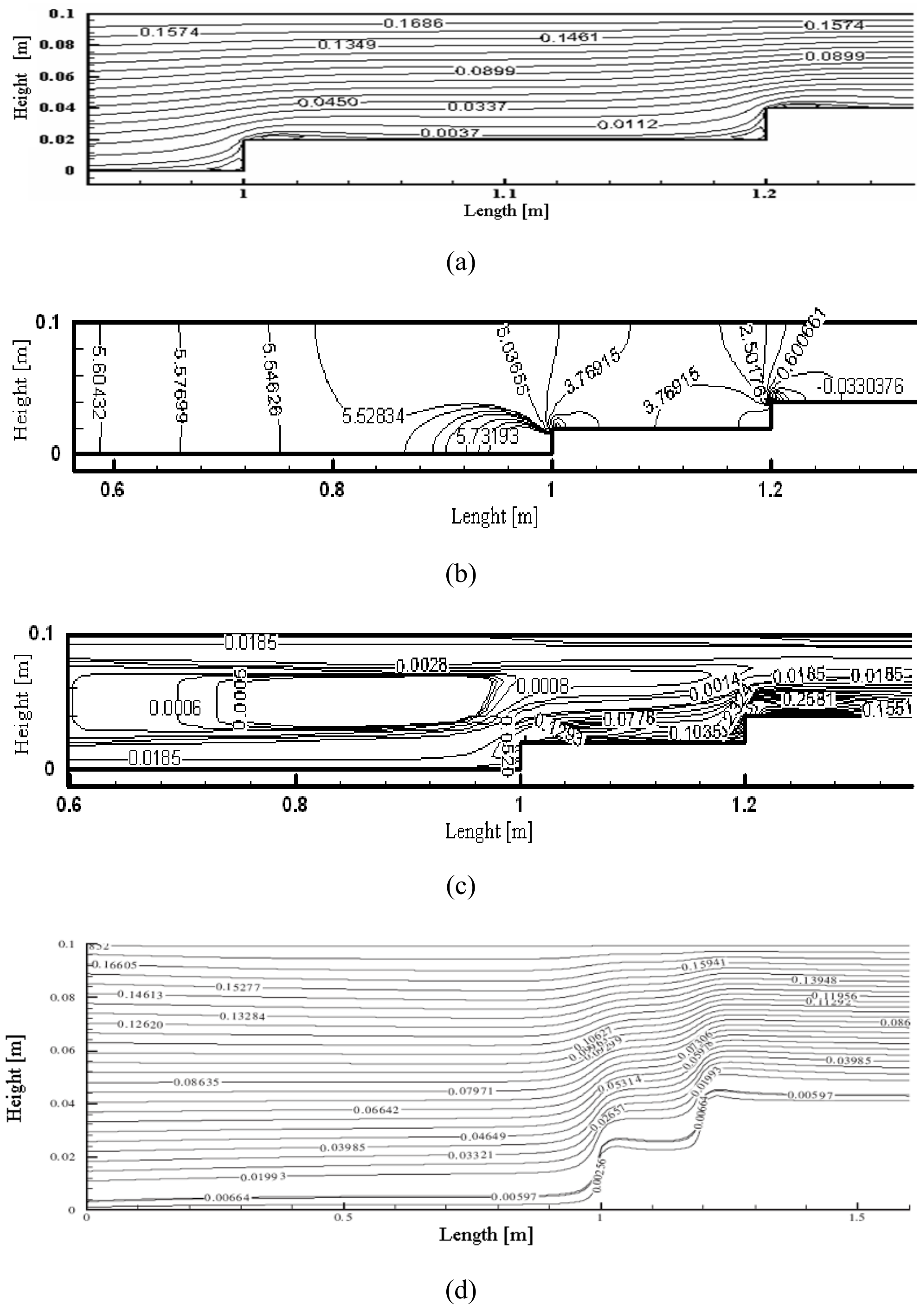

Figure 3. Streamlines, contours of pressure coefficient and turbulent kinetic energy for DFFS flow at Re = 10000 (a) Streamlines, (b) Pressure coefficient, (c) Turbulent kinetic energy and (d) Streamlines, Reference [11].

boundaries and the maximum values occur at the vicinity of the two steps along with a complex variation.

The fluid flow over DFFS was also studied numerically by Yilmaz, et al [11], using commercial FLUENT code. The grid was generated by Gambit pre-processor which was good enough to obtain a grid-independent solution. In order to validate the present numerical procedure, one can compare the computed streamlines in Figure 3a, with those obtained in Reference [11] shown in Figure 3d. Concerning the streamlines and the values of stream function, the present numerical results show good agreement with the theoretical results obtained by the FLUENT code. It should be noted that the x-and y-coordinate axes in Figure 3d have not the same scale factor which makes an apparent difference with Figure 3a. However, it can be concluded that the applied grid generation method based on the Schwarz-Christoffel transformation with the present CFD techniques in solving the governing equations are very powerful and efficient in simulating many turbulent flows with a wide variety of flow geometry.

For the above test case, the influence of grid refinement on the numerical results is also studied. The distribution of x-component of the mean velocity in the duct at axial section before the steps with x = 0.3 m is shown in Figure 4. It is seen that the differences between the predicted velocity distributions on the fine (200×151) and finer (400×151) meshes are fairly small indicating that the numerical results are reasonably grid-independent. A further grid refinement has been undertaken with adding 50 nodes in y-direction but no major change was shown in the computed results. Thereby, results obtained on the (400×151) mesh are regarded as grid-independent.

It should be noted that in the computation of all test cases, the first 20 grid nodes were considered within the region near the wall such that, at the interface between the near wall and fully turbulent region, the value of $y^+ = [y\sqrt{\tau_w/\rho}]/\nu$ was around 50.

In Figure 5, a comparison is made between the present results with experiment and also with the results by DNS method. In this test case, the fluid flow over a right angle, backward facing step in a duct is simulated. The flow condition and geometrical parameters of this test case are given in Reference [12]. Figure 5 shows the variation of skin friction factor, c_f, on the bottom wall after the step surface at Re = 5100. Besides, to show the effect of using linear low-Re turbulence model near the wall region, the results of standard k-ε model without any wall function are also compared with those obtained by linear model for the region near the solid wall. It should be noted that in

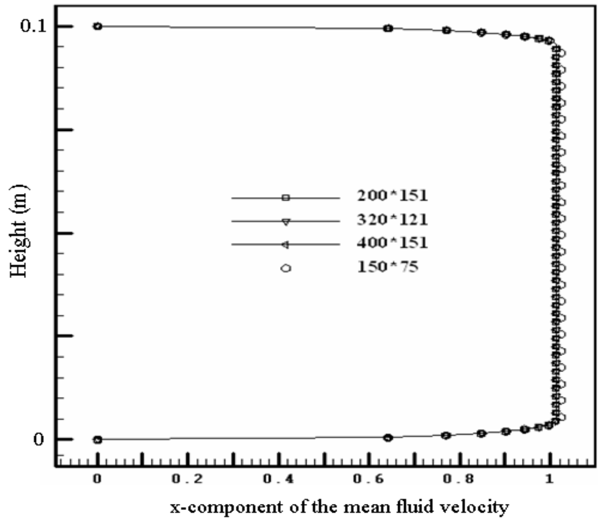

Figure 4. Distribution of x-component of mean velocity in the duct at the axial section x = 0.3 m using four different grid sizes.

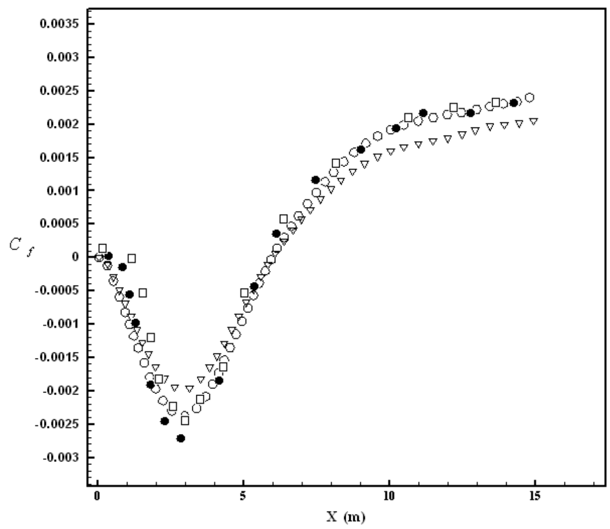

○ Linear low-Re model, ▽ Standard k-ε model
● Experiment [12], □ DNS [12]

Figure 5. variation of skin friction factor on the surface of bottom wall after the step. Re = 5100.

Figure 5, the x-axis starts after the step surface. Figure 5 shows a good consistency between theoretical results with experiment noticing that the results by linear turbulence model are very close to those obtained by DNS method and also with the experiment.

In another test case the turbulent flow over a backward facing step is also simulated and the mean velocity distribution at x = 10.1 cm is shown in Figure 6 and compared with experiment [13]. In the experimental study of Kim, et al [13], the step height was H = 11.43 cm, $H/H_2 = 1.5$ and the value of Reynolds number based on the duct height H, was equal to 1.3×10^5. Figure 6 indicates that the axial section x = 10.1 cm is located in the recirculation zone such that the fluid velocity is negative in the region near the wall. However, the model predictions for the mean velocity appear to be in good agreement with the experiment.

As it was mentioned before, the flow simulation for several other test cases were done in the present study and the results are shown in the following Figures, 7 to 17. Besides, for space saving, the pressure contours and TKE distributions are shown for some of these test cases. Such as the ones for flow over a cylinder, two cubes and car profile, the pressure and TKE contours are plotted in Figures, 10, 13, 14 and 17. These figures indicate small value of pressure and large value for turbulent

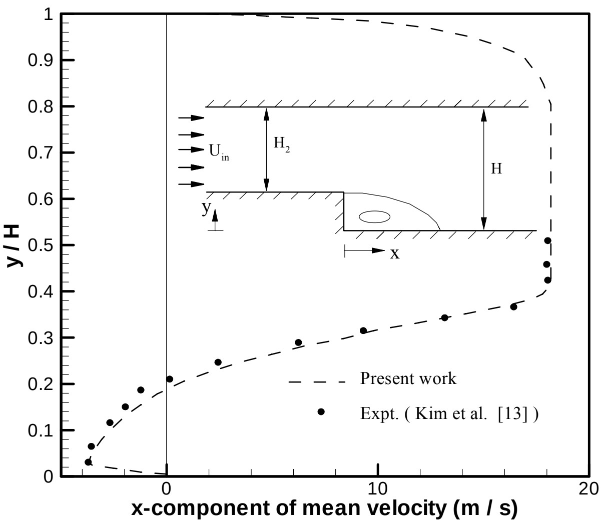

Figure 6. Comparison of mean velocity profile with experiment.

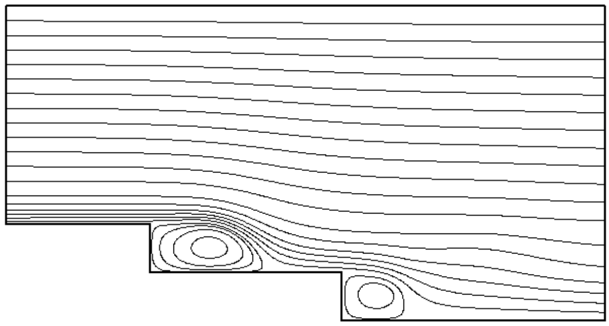

Figure 7. Streamlines for turbulent flow over two backward steps at $Re = 1 \times 10^6$.

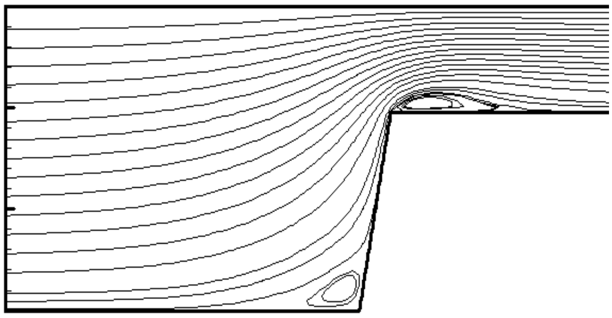

Figure 8. Streamlines for turbulent flow over a forward step with inclination angle of $\theta = 80^\circ$ at $Re = 3 \times 10^4$.

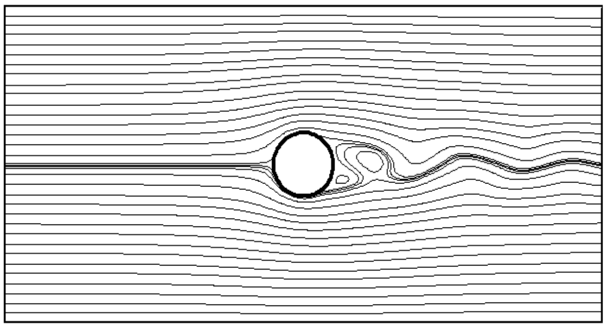

Figure 9. Streamlines for turbulent flow over a cylinder at $Re = 2 \times 10^5$.

kinetic energy in the recirculation zones. The computed streamlines and contours of pressure and TKE are in agreement with literatures, those used different methods in mesh generation and CFD techniques [11-13].

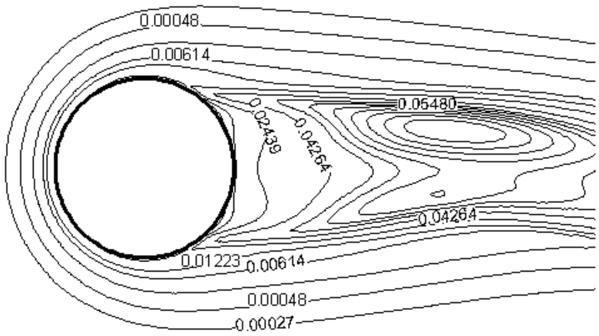

Figure 10. Distribution of TKE for turbulent flow over a cylinder at Re = 2 × 10^5.

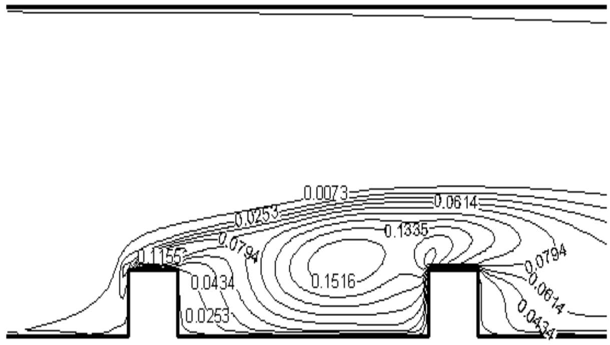

Figure 14. Distribution of TKE for turbulent flow over two cubes at Re = 1 × 10^6.

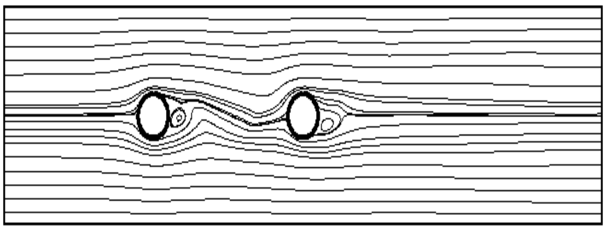

Figure 11. Streamlines for turbulent flow over two cylinders at Re = 2 × 10^5.

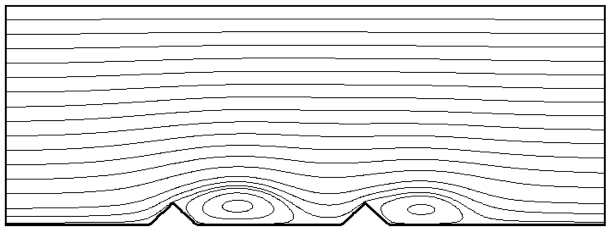

Figure 15. Streamlines for turbulent flow over two sharp bumps at Re = 1 × 10^6.

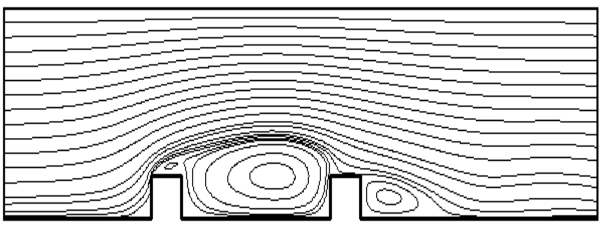

Figure 12. Streamlines for turbulent flow over two cubes at Re = 1 × 10^6.

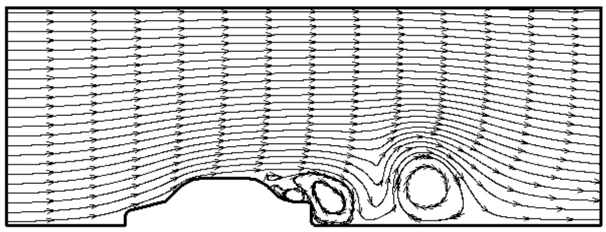

Figure 16. Streamlines for turbulent flow over a car profile at Re = 1 × 10^6.

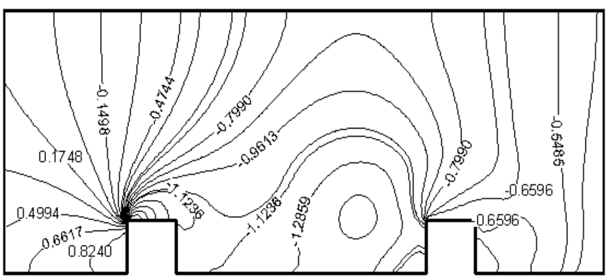

Figure 13. Pressure contours for turbulent flow over two cubes at Re = 1 × 10^6.

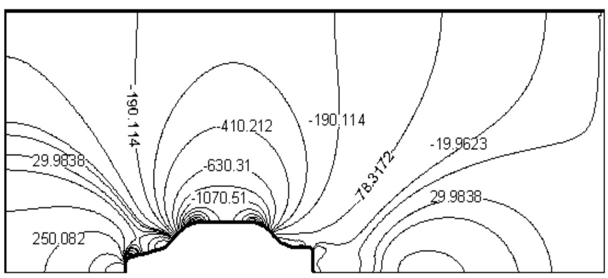

Figure 17. Pressure contours for turbulent flow over a car profile at Re = 1 × 10^6.

6. CONCLUSION

This paper has presented an efficient method based on the Schwarz-Christoffel transformation in generating orthogonal grids for simulation of two-dimensional, incompressible turbulent flows. The governing equations are solved by CFD techniques using the standard k-ε turbulence model in the fully turbulence region and a linear low-Re k-ε model for the region near the solid surface. The transformed forms of the governing equations in the computational domain were discretized with finite volume method and solved by the SIMPLE Algorithm. The model predictions are compared with the available experimental data and a good consistency is found. Thereby, it can be concluded that by the present method, many turbulent flows in different and complex geometries can be simulated accurately.

7. ACKNOWLEDGEMENT

The authors gratefully acknowledge the kind help of Dr. S. M. Hosseini Sarvari in the numerical integration of the Schwarz-Christoffel transformation and orthogonal grid generation.

8. REFERENCES

1. Thompson, J. F., Warsi, Z. U. A. and Mastin, C. W., "Boundary-Fitted Coordinate System for Numerical Solution of Partial Differential Equations", ***A Review, Journal of Computational Physics***, Vol. 47, (1982), 1-108.
2. Sridhar, K. P. and Davis, R. T., "A Schwarz-Christoffel Method of Generating Two-Dimensional flow Grids", ***Journal of Fluid Engineering***, Vol. 197, (1985), 330-337.
3. Moayeri, M. S. and Taghdiri, M. A., "Boundary Conforming Orthogonal Grids for Internal flow Problems", ***Iranian Journal of Science and Technology***, Vol. 17, No. 3, (1993), 191-201.
4. Milne-Thomson, L. M., "Theoretical Hydrodynamics", 4th Edition, Macmillan, New York, U.S.A., (1960).
5. Mansouri, S. H., Hosseini Sarvari, S. M., Keshavarz, A. and Rahnama, M., "An Analytical Numerical Method for Grid Generation by Mathematica", ***Proc. of 26th Annual Iranian Mathematics Conference***, Shahid Bahonar University of Kerman, Kerman, Iran, Vol. 1, (1995), 251-258.
6. Mansouri, S. H., Mehrabian, M. A. and Hosseini Sarvari, S. M., "Simulation of Ideal External and Internal flows with Arbitrary Boundaries using Schwarz-Christoffel Transformation", ***Int. Journal of Eng., Trans. A***, Vol. 17, No. 4, (2004), 405-414.
7. Chowdhury, S. J. and Ahmadi, G., "A Thermohydrodynamically Consistent Rate Dependent Model for Turbulence-Part II. Computational Results", ***Int. Journal of Non-Linear Mechanics***, Vol. 27, No. 4, (1992), 705-718.
8. Yap, C. R., "Turbulent Heat and Momentum Transfer in Recirculation and Impinging Flows", Ph.D. Thesis, Faculty of Technology, University of Manchester, Manchester, U.K., (1987).
9. Raisee, M. and Hejazi, S. H., "Application of Linear and Non-Linear Low-Re k-ε Models in Two Dimensional Predictions of Convective Heat Transfer in Passages with Sudden Contractions", ***Int. Journal of Heat and Fluid Flow***, Vol. 28, (2007), 429-440.
10. Patankar, S. V. and Spalding, B. D., "A Calculation Procedure for Heat, Mass and Momentum Transfer in Three-Dimensional Parabolic Flows", ***Int. Journal of Heat and Mass Transfer***, Vol. 15, (1972), 1787-1806.
11. Yilmaz, I. and Oztop, H. F., "Turbulence Forced Convection Heat Transfer Over Double Forward Facing Step Flow", ***Int. Communication in Heat and Mass Transfer***, Vol. 33, (2006), 508-517.
12. Le, H., Moin, P. and Kim, J., "Direct Numerical Simulation of Turbulent flow Over a Backward-Facing Step", ***J. Fluid Mech***., Vol. 330, (1997), 349-374.
13. Kim, J., Kline, S. J. and Johnston, J. P., "Investigation of Separation and Reattachment of a Turbulent Shear Layer: Flow Over a Backward Facing Step", Report MD-37, Thermo-Science Division, Dept. of Mech. Engng, Stanford University, Stanford, CA, U.S.A., (1978).